Single-Crystal Synchrotron Radiation X-ray Diffraction Study of B and Ga Silicalites Compared to a Purely Siliceous MFI: A Discussion of the Heteroatom Distribution

L. Palin[†] and C. Lamberti

Dipartimento di Chimica IFM, Università di Torino, Via P. Giuria 7, I-10125 Torino, Italy and INFM U.d.R. di Torino Università

Å. Kvick

ESRF, BP 220, F-38043 Grenoble Cedex, France

F. Testa and R. Aiello

Dipartimento di Ingegneria Chimica e dei Materiali, Università della Calabria, I-87030 Rende (Cs), Italy

M. Milanesio* and D. Viterbo

Dipartimento di Scienze e Tecnologie Avanzate, Università del Piemonte Orientale A. Avogadro, Corso T. Borsalino 54, I-15100 Alessandria, Italy

Received: November 29, 2002; In Final Form: February 19, 2003

We report the structure determinations, obtained by synchrotron radiation single-crystal X-ray diffraction experiments, of as-synthesized orthorhombic MFI boron and gallium silicalites compared to that of an unsubstituted defect-free silicalite. The synthesis in fluoride medium yielded comparatively large twinned single crystals. The absence of any measurable signal due to Si(OH) species in the ^{29}Si NMR spectra of silicalite (Fonseca, A.; Nagy, J. B.; El Hage-Al Asswad, J.; Mostowicz, R.; Crea, F.; Testa, F. *Zeolites* **1995**, *15*, 259) indicates that their defectivity is very low because these samples are almost free of Si vacancies, which are usually rather common in MFI materials. All carbon and nitrogen atoms of the disordered tetrapropylammonium (TPA^+) template molecules have been located. These molecules, located at the intersection of the straight and sinusoidal channels, are similar to those found by Van Koningsveld et al. (Van Koningsveld, H.; Van Bekkum, H.; Jansen, J. C. *Acta Crystallogr., Sect. B* **1987**, *34*, 127) in the parent ZSM-5 system. The presence of residual electron density peaks near the T9 and T10 sites in the silicalite sample, similar to those found in Fe-silicalite (Milanesio, M.; Lamberti, C.; Aiello, R.; Testa, F.; Piana, M.; Viterbo, D. *J. Phys. Chem. B* **2000**, *104*, 9951) and consistent with the recent NMR results (Fyfe, C. A.; Brouwer, D. H.; Lewis, A. R.; Chezeau, J. M. *J. Am. Chem. Soc.* **2001**, *123*, 6882), indicate the presence of a SiO_4F^- group at T9 and also at T10. Refinement of the occupation factors of the T sites indicates that a random distribution of B and Ga atoms in the MFI framework is important, even if a certain degree of preferred substitution does exist (T1 for B and T2 for Ga). Synchrotron radiation XRD powder data on defect-free silicalite and Ga-substituted silicalite confirm the single-crystal results, indicating that they are not biased by twinning.

1. Introduction

Silicalite, first synthesized at the Union Carbide laboratories by the Flanigen group,[1] is an aluminum-free zeolite with the MFI structural topology.[2] It shows a 3D pore system consisting of two intersecting sets of tubular channels, a linear one parallel to the [010] direction, with an opening of approximately 5.4 × 5.6 Å^2, and a sinusoidal one parallel to the [100] direction, with an opening of 5.1 × 5.5 Å^2.[3,4] Both channels are defined by 10-membered rings of SiO_4 tetrahedra (T sites in Figure 1). The isomorphous substitution of Si by other tetrahedrally coordinated heteroatoms such as B^{III},[5,6] Al^{III} (ZSM-5),[3] Ti^{IV} (TS-1),[7] Ga^{III},[8,9] and Fe^{III} [10] in small amounts (up to 2−3 wt %) provides new materials showing specific catalytic properties in oxidation and hydroxylation reactions related to the coordination state of the heteroatom.[11] Moreover, MFI-type materials with trivalent metals present in tetrahedral (T) sites have had a tremendous impact as new shape-selective industrial catalysts having tunable acidic strength. In fact, the acidic strength of the protons in the bridged $Si(OH)M^{III}$ (M = B, Al, Fe, Ga) groups depends on the nature of the trivalent heteroatom. Indeed, the choice of M(III) critically affects this acidity property according to the sequence Al > Fe ≈ Ga ≫ B.[12] The recent discovery of an Al-containing natural zeolite (mutinaite) with the MFI topology[13] also makes this structure relevant to the mineralogical field.

It is worth noting that silicalite samples with very different morphologies, crystal quality, and dimensions can be obtained using different synthesis conditions. Silicalites synthesized following the original recipe[1] in hydroxyl media have well-defined crystallites with a size of 2−3.5 μm and *Pnma*

* Corresponding author. E-mail: marco.milanesio@mfn.unipmn.it. Fax: +39-0131-287416.

[†] Present address: ESRF, BP 220, F-38043 Grenoble Cedex, France.

10.1021/jp027586r CCC: $25.00
Published on Web 04/04/2003

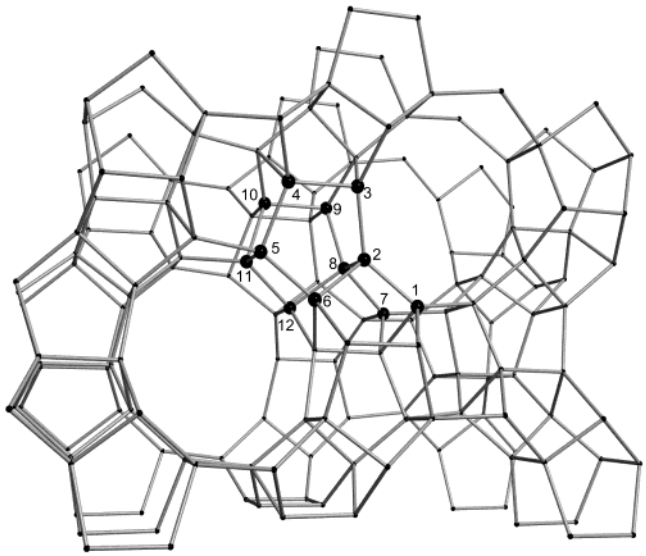

Figure 1. Representation of the MFI framework, seen through the straight channel, with the labeling scheme of the 12 independent T sites.

orthorhombic symmetry. After calcination, the symmetry changes to monoclinic $P2_1/n$. On chemical grounds, they have Al and Na impurities and show a very low density of internal defects (i.e., Si vacancies). Silicalites synthesized in Na-free hydroalcohol media[14] have a significantly smaller crystal size (0.2−0.3 μm), yielding a high-surface-area powder with a much lower level of impurities but a much higher density of internal defects.[14−17] The lack of one or more adjacent silicon atoms in these defects is balanced by the presence of hydroxylated nanocavities in the framework, also referred to as hydroxyl nests. The absence of impurities and the presence of internal hydroxyl nests have significant consequences on the long-range structural order. Indeed, samples prepared as described in ref 14, after calcination, maintain orthorhombic *Pnma* symmetry.

In the past decade, a large number of studies aiming at a systematic characterization of metal-substituted MFI materials have been reported. From the crystallographic point of view, even though the structure of the hosting MFI matrix has been satisfactorily clarified, the distribution of the heteroatoms over the 12 symmetry-independent T sites of the orthorhombic MFI framework (Figure 1) is still open to debate. In particular, it is not clear if the heteroatom distribution among the T sites may depend on the heteroatom type (Al^{III}, B^{III}, Ti^{IV}, Ga^{III}....) and/or on the synthesis method (e.g., from fluoride or hydroxyl media). This is an important problem because the localization of the heteroatoms may play an important role in understanding the catalytic properties of the material. The low fraction of heteroatoms that can be inserted into the MFI framework (up to 2−3 wt %) makes the experimental localization of these atoms by diffraction measurements very difficult. For this reason, most speculations concerning the substituted silicalites have been based on computational chemistry results,[18−20] which all agree in giving small energy differences for heteroatom substitution in different T sites. Only a few crystallographic studies have been reported. Among those, we shall recall synchrotron radiation powder XRD analyses on TS-1,[21,22] a synchrotron radiation single-crystal XRD study on Fe-silicalite,[23] and powder neutron diffraction studies on TS-1[20,24,25] and on Fe-silicalite.[20] Both theoretical[18,20] and experimental[20−25] investigations give rather contradictory results for the location of the heteroatoms. A powder neutron diffraction characterization of defective silicalite has recently been reported by Artioli et al.,[16] showing that T vacancies do not occur randomly but are preferentially located at sites T6, T7, T10, and T11 (Figure 1). In our single-crystal study of Fe-silicalite,[23] the location of Fe^{III} at sites T9 and T10 was suggested. It is evident that a precise crystallographic study of the reference material (i.e., pure and defective-free silicalite) could be of great help in validating the faint experimental evidence used by different groups to support the assertions made in the above summarized papers.

We describe here a synchrotron radiation XRD study of as-synthesized orthorhombic MFI boron and gallium silicalites (hereafter B-MFI and Ga-MFI, respectively) compared to an unsubstituted, defect-free silicalite (hereafter pure MFI). B and Ga atoms have respectively smaller and larger atomic numbers and van der Waals dimensions with respect to the Si atom, and in general, B and Ga insertion into the T sites should cause opposite structural changes. The comparison between B-MFI and Ga-MFI data should enhance any preferential substitution effect, even though there is no a priori reason that the preferred substitution sites are identical for B and Ga. Moreover, in this work, we have also collected X-ray data on a pure and defect-free silicalite, which is a perfect reference material.

The silicalite single crystals were grown in fluoride media and exhibit comparatively large dimensions (~25 × 40 × 110 μm^3) with respect to those obtained by the Flanigen method.[1] These crystals, synthesized as described in ref 26, are twins. ^{29}Si solid-state NMR studies[27] showed only the chemical shift due to $Si(OSi)_4$ whereas no $SiOH(OSi)_3$ signal was detected, indicating that Si vacancies are virtually absent in this material. This structural study can then be considered to be complementary to the previous work by Artioli et al.[16] on defective silicalite. More recently, Aubert et al.[28] published a single-crystal study of silicalite-1, underlining the presence of F atoms near T9 in the structure. The presence of 5-fold-coordinated $[SiO_4F^-]$ sites[29] has also been singled out in the detailed NMR studies by Koller et al.[30] and Fyfe et al.[31]

Because template burning, even under mild conditions, causes a partial degradation of crystal quality[32] and may cause heteroatom migration from framework T sites,[8c,d,10b−d] we were forced to perform this diffraction study on the as-synthesized crystals containing the tetrapropylammonium (TPA^+) template. The aim of this study is to locate structurally the various moieties (MFI framework, TPA^+, and F^-, B, or Ga heteroatoms) that contribute to the formations of the MFI precursor, paying particular attention to the charge distribution and balance of the whole structure. High-resolution synchrotron radiation XRD powder diffraction data were also collected to confirm that the single-crystal analyses are not affected by twinning. A detailed description of the X-ray powder data analyses will be reported in a separate paper.[33]

2. Experimental Section

2.1. Sample Synthesis. Pure MFI was prepared from a synthesis mixture having the following molar composition: 1:10:2:500 $KF/SiO_2/TPABr/H_2O$. In a typical preparation, 0.94 g of KF was dissolved in 40 g of distilled water. At the same time, 5.32 g of TPABr (tetrapropylammonium bromide) was dissolved in 41 g of distilled water. The two solutions were mixed. Finally, 15 g of colloidal silica LUDOX HS-40 was added. The resulting clear solution was put in a 25-cm^3 Morey-type PTFE-lined autoclave. Hydrothermal treatment was carried out in a thermoventilated oven at 170 °C for 48 h. The unit-cell contents of TPA^+ and F^- were 3.8 and 2.2, respectively.

The B-MFI sample was synthesized according to the method reported in ref 34. The composition of the initial mixture was

TABLE 1: Summary of Crystal Data for the Three Investigated Samples

compound	pure MFI	Ga-MFI	B-MFI
crystal size (μm)	120 × 60 × 40	80 × 40 × 20	140 × 70 × 50
a	20.042(3) Å	20.04(1) Å	19.968(3) Å
b	19.990(3) Å	20.02(1) Å	19.955(3) Å
c	13.414(2) Å	13.433(7) Å	13.372(2) Å
V	5374(1) Å^3	5389(5) Å^3	5328(1) Å^3
total measured reflections	14 932	58 963	28 218
observed reflections ($I > 2\sigma(I)$)	3389	4102	4462
data/restraints/parameters	6348/36/351	7411/36/351	6419/36/351
GOF on $\|F_o\|^2$	1.11	1.01	1.02
R indices [$I > 2\sigma(I)$]	R1 = 0.0593	R1 = 0.0572	R1 = 0.0429
	wR2 = 0.1274	wR2 = 0.1203	wR2 = 0.0979
R indices (all data)	R1 = 0.1103	R1 = 0.1015	R1 = 0.0643
	wR2[a] = 0.1456	wR2[a] = 0.1289	wR2[a] = 0.1030
largest diff peak and hole	0.688, −0.843 e Å^{-3}	0.560, −0.860 e Å^{-3}	0.606, −0.580 e Å^{-3}

[a] Weight calculated according to $w = 1/[\sigma^2(|F_o|^2) + (P)^2]$, where $P = (|F_o|^2 + 2|F_c|^2)/3$.

9:0.5:10:1.25:330 $KF/H_3BO_3/SiO_2/TPABr/H_2O$. The unit-cell contents of B, TPA^+, and F^- were 2.2, 3.6, and 1.4, respectively.

The Ga-MFI sample was synthesized according to the method reported in ref 35. The composition of the initial mixture was 12:0.3:10:1.25:330 $NaF/Ga(NO_3)_3/SiO_2/TPABr/H_2O$. The unit-cell contents of Ga, TPA^+, and F^- were 1.8, 3.8, and 1.2, respectively.

2.2. Data Collection. From all of the above syntheses, crystals of comparatively large dimensions ($\sim 20 \times 30 \times 100\ \mu m^3$) were obtained. The crystals are twins, but the twin law could be easily found from the violations of the systematic absences expected for the *Pnma* space group. The twinning is due to a 4-fold twin axis along the [001] direction.[36−38]

Single-crystal diffraction measurements were carried out on pure MFI and on Ga- and B-MFI samples at the ID11 beamline[39] of the European Synchrotron Radiation Facility operating at $\lambda = 0.44480$ Å and using a Bruker CCD detector. The reduction of the single-crystal data was carried out using the SMART[40] and SAINT[41] programs. To account for a slight spot splitting at high angles due to the twinning, the data reduction was performed using a comparatively large integration box. The most relevant crystal data are reported in Table 1.

2.3. Structure Refinements. Using as a starting model the *Pnma* structure of ZSM-5 determined by Van Koningsveld et al.,[42] we carried out the refinement of all three structures by full-matrix least squares and difference Fourier recycling using the SHELXL-97 program,[43] which is capable of handling data from twinned crystals. Graphical output and manipulation have been generated using MOLDRAW software.[44] All 12 T sites were occupied by Si atoms only. The location of the disordered TPA^+ template in all of the crystals was then determined by several difference Fourier cycles, and the refinement of the template atoms was carried out using isotropic displacement parameters and geometrical restraints on bond distances and angles. The occupancies of the TPA^+ disordered atoms were found by refining the site occupation factors (SOF) while keeping the ADPs fixed. This approach allowed us to compare the occupancies of the template in our samples with those obtained by Van Koningsveld et al.[42] on ZSM-5 and by us on Fe-MFI.[23] To determine whether the TPA^+ structure and F^- distribution could be consistent with lower symmetry with no mirror plane at $y = {}^1/_4$ (relating unprimed and primed atoms in Figure 3), we also carried out the refinement in the $Pn2_1a$ space group. This indeed yielded a better TPA^+ structure, but the refinement of the MFI framework was not stable, indicating that the framework must obey *Pnma* symmetry. Conversely, the F^- distribution is not affected by the absence of the mirror plane.

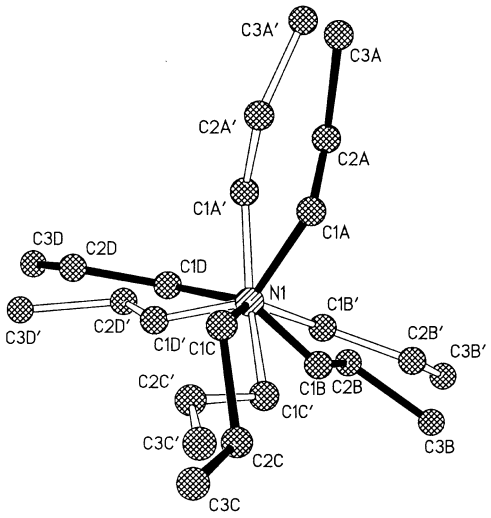

Figure 2. Superposition of the two components of the disordered TPA^+ structure. The solid black bonds indicate the major component ($^2/_3$ population).

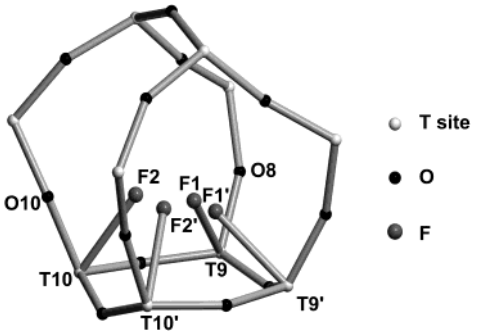

Figure 3. Picture of the cage with the possible 5-coordinate SiO_4F^- groups at sites T9 and T10, obtained from the refinement of single-crystal X-ray data.

Once both the framework and the TPA^+ were refined, a significant electron density peak (Table 2) close to T9 was still found in the difference Fourier map. In a subsequent refinement cycle, according to Aubert et al.,[28] we introduced this peak as a fluorine atom.

At this stage of the refinement, we attempted to shed some light on the B or Ga distributions among the 12 T sites. To get a uniform situation, in all subsequent refinement cycles we fixed the overall template population to the theoretical value of 4.0 molecules/unit cell, thus refining the corresponding ADPs. The completion of the refinement is not straightforward and will be discussed in detail in Results and Discussion.

TABLE 2: TPA^+, F^-, and Heteroatom (M = Ga or B) Content Per Unit Cell[a]

sample	$TPA^{+(a)}$	$F^{-(a)}$ (x)	$M^{(a)}$ (y)	F1 peak[(b)]	F2 peak[(b)]	F1 SOF[(c)]	F2 SOF[(c)]	$F^{-(d)}$
pure MFI	3.8	2.2		1.69	1.05	0.23(1) [0.23(1)]	0.04(1) [NO]	2.2(1)
Ga-MFI	3.8	1.2	1.8	1.31	0.63	0.25(1) [0.24(1)]	0.06(1) [NO]	2.5(1)
B-MFI	3.6	1.4	2.2	0.69	NO	0.101(6) [NA]	0.018(5) [NA]	0.95(6)

[a] From elemental analysis [4, x and y in eq (2) respectively]. [b] Height of fluorine peaks (in e^-/A^{-3}) near T9 (F1) and near T10 (F2); note that for Fe-MFI the electron density of F1 and F2 peaks was 2.38 and 0.67 e^-/A^{-3}, respectively.[23] [c] Refined site occupation factors (SOF); in square brackets the SOF from Rietveld refinement of powder data; NA = data not available, NO = not observed peak. [d] Total F^- content in the unit cell, from crystallographic data.

3. Results and Discussion

3.1. Refinement of the Three Structures as Siliceous MFI. At first, all three samples in Table 1 were refined with the same structural model (a pure SiO_2 MFI framework with a disordered TPA^+ molecule). The disordered template must be located with great precision to be sure that the remaining significant electron density peaks can be correctly interpreted. The high quality of the single-crystal data obtained at beamline ID11 of ESRF allowed for a good elucidation of the TPA^+ structure, which is consistent with that found in ZSM-5[42] and in Fe-silicalite,[23] even if some minor differences in the occupation factors of the C atoms were observed. The template molecules are located at the intersections of the straight and the sinusoidal channels. The N atom lies on the mirror plane at $y = {}^1/_4$, and two distinct disordered positions of the tetrahedral arrangement of the propyl arms are obtained. It has also been possible to estimate the ratio between the populations of the major and minor disordered positions of TPA^+ (represented in Figure 2), which resulted in about ${}^2/_3$ and ${}^1/_3$, respectively, in all three samples. In Table 1, a significant decrease in the cell volume ($\Delta V = -46(1)$ Å^3) is observed on passing from pure MFI to B-MFI, in keeping with the decrease reported by Millini et al.[45] in samples with increasing B content. This indicates a comparatively high degree of insertion of the smaller B in the MFI framework. On the contrary, the small volume increase observed for Ga-MFI is hardly significant. Indeed, the correlation between the cell volume and the heteroatom size and content does not always apply because different T−O−T angular distortions for different heteroatoms may counterbalance the size effect, as in the case of Ga-SOD.[46] Finally, we note that the values of the cell volumes may be affected by an additional systematic error because they are derived from twinned crystals.

As mentioned in section 2.3, after the refinement of both the framework and TPA^+, a significant residual electron density peak near T9 was found. The interpretation of this extraframework peak is fundamental to the understanding of the nature of these silicalites synthesized in fluoride media. The presence of this peak in pure MFI, similar to that found in Fe-silicalite,[23] disagrees with our previous interpretation of this peak being due to the alkaline counterion. Indeed, a recent extended NMR analysis[31] has unambiguously demonstrated that at site T9 a 5-coordinate SiO_4F^- group (F1 in Figure 3) is present in silicalite crystals prepared in fluoride media. As first indicated by Aubert et al.,[28] the residual electron density peak should therefore be interpreted as being due to the fluoride anion linked to the T9 site located in a four-membered ring, where F^- may stabilize the strained Si−O−Si bonds. The formation of a 5-coordinate group also explains the observed lengthening of the T9−O average distance (Figure 4). The residual electron density was then carefully analyzed to locate other possible 5-coordinate SiO_4F^- groups in the remaining 11 T sites, and only a small peak near T10, named F2, was found. (See Table 2 and Figure 3.)

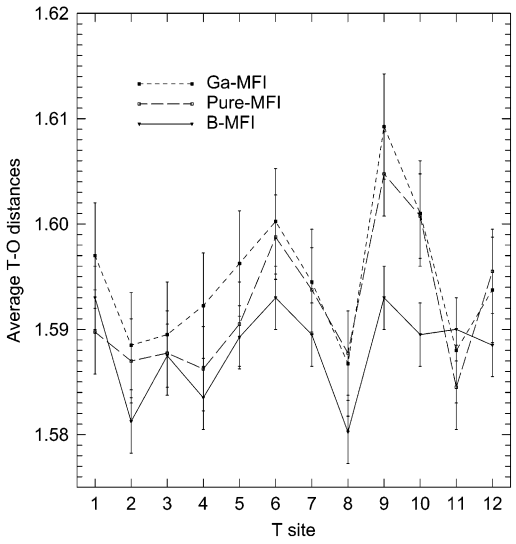

Figure 4. Average T−O distances in B- and Ga-MFI compared to those of pure MFI.

The F1 location near the twinning axis might be affected by the twinning in the single-crystal analysis. To verify this point, Rietveld analysis of the powder data collected on the same pure MFI sample at beamline BM16 of ESRF was carried out by means of the GSAS software,[47] employing as starting model the results of the pure MFI single-crystal refinement. The F1 SOF refined in this way confirmed that single-crystal results are not biased by twinning. (See Table 2.)

Refinement of the fluorine occupation factors in the $Pn2_1a$ space group indicated that F1 and F1′ SOFs remain practically identical, even when the $y = {}^1/_4$ mirror plane of the *Pnma* space group is removed, confirming that F1 and F1′ (Figure 3) are really equivalent sites. The same holds for F2 and F2′. Figure 3 shows all four possible fluorine sites, but obviously only one fluorine position can be occupied in any given cage at any given time. The NMR study of Koller et al.[30] suggested that fluorine ions should jump between more than two (not defined) sites. Successively, Fyfe et al.[31] clearly demonstrated, again from NMR data, that the fluorine ions jump between the mirror-related F1 and F1′ sites (according to our notation in Figure 3). Thanks to the accuracy of our X-ray data, we were able to show that fluorine can also occupy sites F2 and F2′ near T10 (Figure 3). Even though we have no direct indication of the dynamic behavior of the fluorine atoms, the short distances (<1.3 Å) separating F1, F1′, F2, and F2′ (with F1−F2 ≈ F1−F1′ ≈ F2−F2′) and the overlap of the corresponding electron density peaks suggest that jumps can occur not only between F1 and F1′ but

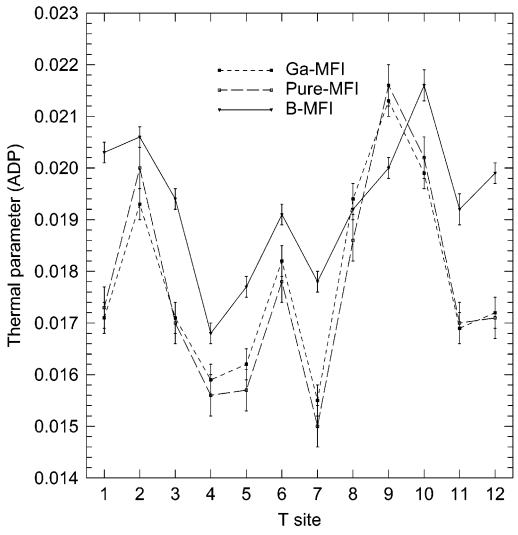

Figure 5. Atomic displacement parameters (ADPs) of B- and Ga-MFI compared to those of pure MFI, obtained by assuming that the T sites are fully occupied by Si during the single-crystal X-ray data refinement.

also between all four sites in Figure 3. Sites F1 and F1′ are more populated because they are less sterically hindered.

Starting from this common point, we began to analyze the effects of heteroatom insertion in the MFI framework. Indeed, B, Si, and Ga atoms, with quite different atomic numbers (Z = 5, 14, and 31, respectively), have significantly different X-ray atomic scattering factors and ionic radii; therefore, it can be expected that their insertion in the MFI framework is detectable by X-ray diffraction techniques. Indeed, some significant differences between substituted and unsubstituted silicalites arise when a careful analysis of the average T−O distances (Figure 4) of ADPs (Figure 5) and of SOFs (Figure 6) of the 12 T sites is performed.

The analysis of the trend in the T−O distances (averaged over the 4 bonds of the TO_4 unit) in the 12 independent tetrahedral sites is shown in Figure 4 for pure MFI, B-MFI, and Ga-MFI. It may be seen that site T9 has the largest T−O average distance in pure MFI and Ga-MFI, similar to what is observed in Fe-silicalite[23] (also prepared in fluoride medium). This observation is in agreement with the formation of a 5-coordinate SiO_4F^- group[29] at T9 in pure MFI (vide infra). Indeed, in the trigonal bipyramid around T9, a significant lengthening of the axial T−O distance opposite to the F^- anion is the main result of the overall lengthening of the average T9−O distance.[28,31]

Because of the differences in the weight and dimensions between B, Si, and Ga, the heteroatom insertion should induce some observable effects in the ADP of the T sites when the refinement is carried out by assuming that all T sites are fully occupied by Si atoms. Indeed, looking at Figure 5, we clearly see that in B-MFI the T sites present ADP values that are systematically larger than those of pure MFI whereas in Ga-MFI the differences in the ADPs with respect to pure MFI are within the experimental errors. The ADP values, averaged over the 12 sites, are 0.0193(2), 0.0177(3), and 0.0178(3) Å^2 for B-MFI, pure MFI, and Ga-MFI, respectively. Inserting the smaller and lighter B atoms may cause some disorder and a decrease in electron density at the T sites. Both effects cause, in the adopted refinement strategy, an increase in the ADPs, which is clearly detectable in Figure 5. Conversely, Ga insertion has two contrasting effects: (i) the larger dimension of Ga with respect to Si may cause distortions resulting in an increase of the ADPs and (ii) the larger atomic number of Ga causes an increase in the electron density of the T site, which induces smaller ADP values. It is worth noting that all T sites in B-MFI present an increase in their ADP values, with the only exception being T9. This is the first indication that a significant degree of B insertion occurs in all T sites. Nevertheless, some T sites present larger deviations, suggesting a certain degree of preferential substitution, which will be discussed further in section 3.3. For pure MFI and Ga-MFI, T9 shows the largest ADP deviation with respect to the value averaged over the 12 sites because of the presence of the fluorine atoms. (See the next paragraph and Figure 3.) Indeed B-MFI, where the occupation factor of fluorine is smaller (see Table 2), does not show the large thermal factor increase for T9 observed for pure MFI and Ga-MFI (see Figure 5).

3.2. Charge Balance in the MFI Samples. The correct interpretation of the extraframework peaks in the electron density maps may also shed some light on the charge distribution and balance in these silicalite samples. A perfect SiO_2 MFI framework is neutral whereas the TPA^+ template molecules induce the presence of about 4 positive charges in the unit cell (a little bit less from elemental analysis, see Table 2). The elemental analysis indicates that cations such as Na^+ and K^+ are present in pure MFI and B- and Ga-MFI with a concentration lower than 0.2% and their small contribution can be accounted for in the charge balance if we assume 4 positive charges/unit cell. Fluorine ions donate to the MFI framework some of the negative charges needed to achieve electric neutrality. In the pure-MFI case, the synthesis is carried out at high pH, and OH^- ions from TPAOH may contribute to the charge balance. Trivalent heteroatoms such as B^{3+} and Ga^{3+}, substituting for a Si^{4+} atom in the framework, also play the same role. Therefore, the population of the F^- anion and the location of the heteroatoms in the framework are fundamental to the understanding of the charge balance in the as-synthesized MFI samples. The very small number of defects in pure MFI, synthesized in fluoride media,[27] allows the exclusion of defects from the charge balance, but they are relevant for B- and Ga-MFI, where because of the lower pH of the synthesis mixture, the presence of OH^- ions from TPAOH can be excluded. Indeed, the number of defects (about 1 per unit cell) is certainly low but nevertheless important in the final charge balance as described below. Vacancies are certainly more important in the charge balance of silicalites synthesized by other methods.[1,14]

Therefore, in defect-free pure MFI, where the SiO_2 stoichiometry is respected and no internal SiOH groups are detected, the charge-balance equation is

$$4[TPA^+] = x[F^-] + (4 - x)[OH^-] \qquad (1)$$

As we have seen, fluoride ions are mainly located near sites T9 and T10, confirming that only the small and strained four-membered rings, where the tetrahedral coordination of Si is most distorted, are able to link the fluorine atoms, in agreement with the result of George and Catlow.[48] To explain the larger population of F1 with respect to that of F2 (see Table 2), we explored the environment of the two fluorine positions. By analyzing the shortest contacts between the fluorine atoms and the neighboring oxygens, it can be seen that all of the F1−O contacts in the cage depicted in Figure 3 are longer than 2.1 Å but that F2 is involved in a contact with O10 of less than 1.8 Å. We may conclude that F2 insertion causes a greater distortion in the framework than F1 insertion; therefore, the stability and population of F2 are smaller than the values for F1.

The insertion of F^- anions in the first coordination shell of Si implies a transition from a tetrahedral-like geometry to a bipiramidal-like geometry. This transition is favored in the T sites exhibiting, on their own, a larger deviation from the ideal local tetrahedral geometry.[49] In the MFI framework, the larger deviation from T_d symmetry occurs for T9 and T10, which are the only ones forming a four-membered ring. Bonding of F atoms to the remaining 10 T sites would require a significantly larger cost and therefore is unfavorable.

In the pure-MFI sample after single-crystal refinement, there are 4.0 TPA^+/unit cell and about $x = 2.0$ F^-/unit cell, considering both extraframework peaks near T9 and T10. The remaining negative charge could be carried by OH^- groups that are highly disordered and impossible to locate by X-ray diffraction.

In B- and Ga-MFI, the charge balance is slightly complicated by the presence of a trivalent heteroatom in the framework. NMR data from Nagy et al.[27] suggest that our B- and Ga-MFI crystals present a small but still detectable number of defects (about 1 per unit cell), and the charge balance equation can be written as

$$4[TPA^+] = x[F^-] + y[M^{3+}] + (4 - x - y)[\text{defects}] \quad (2)$$

where M = B or Ga and the corresponding x and y values are reported in Table 2. For B- and Ga-MFI, it can be seen that $x + y \approx 3$; therefore, the defect contribution is about 1 per unit cell, which is comparable with the value suggested from NMR analysis.[27]

The amount of F^- estimated by XRD analysis is reported in the last column of Table 2. A comparison of XRD and elemental analysis values shows good agreement for pure MFI and B-MFI but a significant deviation for the Ga-MFI sample. An analysis of the F^- occupancy in Table 2 indicates that in B-MFI, where the B content is a little larger, the residual electron density peak near T9 is much smaller than in pure MFI and at the same time no lengthening (see Figure 4) of the T9−O distances is observed. Indeed, in B-MFI, the lengthening due to the limited formation of 5-coordinate groups might be well compensated by the shortening due to B insertion, and the result is a T9−O average distance that is shorter than that in pure MFI and similar to that in ZSM-5.[42]

In Ga-MFI, the F^- population is similar to that of pure MFI. The Ga atom is larger than Si, and its insertion is expected to cause a small lengthening of the T−O distance. As far as T9 is concerned, this small effect is dominated by the larger lengthening due to F^- insertion. As a result, the average T9−O distance in Ga-MFI is only slightly larger than that in pure MFI. Similar behavior was also observed in Fe-silicalite.[23]

3.3. Refinement of the Site Occupation Factors of the T Sites. Different groups[16,20−22,24,25,50] proposed a number of ways to find some indication of the heteroatom distribution among the 12 T sites of the MFI framework (Figure 1) from diffraction data. Indeed, the attempt at determining the x_i occupancy factor of the heteroatom in the ith T site ($1 - x_i$ being the Si occupancy and $i = 1-12$) is extremely critical because of the small amount of substitution and the strong correlation between x_i and the corresponding ADP. Three main strategies have been proposed to overcome this problem: (i) Lamberti et al.,[24] using neutron powder diffraction data for TS-1, refined x_i of Ti and a common thermal parameter for all T sites with chemical constrains on the total number of Ti atoms in the structure; (ii) Hijar et al.[20] and Henry et al.,[25] also using neutron powder data, refined the occupation factors of the T sites (treated as Si atoms) and a common thermal parameter; (iii) Zanardi et al.,[50] using single-crystal X-ray data on B-FER, alternatively refined SOFs and ADPs of the Si and B atoms until self-consistency was achieved.

TABLE 3: Refined SOFs of the T Sites Treated as Si Atoms in the Three Structures

T site	SOF (B-MFI)	SOF (pure MFI)	SOF (Ga-MFI)
T1	0.883(3)	0.909(4)	0.921(4)
T2	0.898(3)	0.897(4)	0.932(4)
T3	0.898(3)	0.916(4)	0.925(4)
T4	0.900(3)	0.924(4)	0.933(4)
T5	0.911(3)	0.924(5)	0.933(4)
T6	0.906(3)	0.909(4)	0.928(4)
T7	0.911(3)	0.924(4)	0.941(4)
T8	0.897(3)	0.910(4)	0.913(4)
T9	0.884(3)	0.900(5)	0.919(4)
T10	0.886(3)	0.902(4)	0.920(4)
T11	0.901(3)	0.923(5)	0.930(4)
T12	0.889(3)	0.901(4)	0.926(4)

In the present work, we exploited the fact that we have not only collected synchrotron radiation single-crystal data but have also carried out the analysis of a perfect reference material (i.e., the defect-free pure MFI). We first used the pure MFI data to obtain the ADPs of the Si atoms in a purely siliceous MFI framework (dashed line in Figure 5). The SOFs of the T sites, treated as Si atoms, were at first refined, fixing the ADPs to the pure MFI values for all three structures, thus neglecting the effects of heteroatom and fluorine content on the ADP of each T site. Then, the SOFs and ADPs of the Si atoms were refined separately in alternate cycles until self-consistency was achieved. Different restraints on the disordered TPA^+ moiety were also used, but the final refined SOFs of the T sites (reported in Table 3) were not affected by this different TPA^+ modeling within esd's. The resulting refined SOFs are all less than 1 for pure MFI because of the positive charge carried by Si in the SiO_4 tetrahedra. The average Si SOF is 0.912, resulting in an average charge of $+1.2|e|$, a value in keeping with the results of theoretical ab initio calculations both on a cluster and a periodic system.[51] The most relevant result derivable from Table 3 is the validity of the following inequality:

$$\text{SOF(B-MFI)} < \text{SOF(pure MFI)} < \text{SOF(Ga-MFI)} \quad (3)$$

Equation 3 holds for all of the 12 T sites. The only insignificant exception occurs for T2, where SOF(B-MFI) = 0.898(2) and SOF(pure-MFI) = 0.897(4). For most sites, the inequality (eq 3) holds with a confidence level higher than 2σ. Therefore, the differences in the electron density of the T sites, induced by the heavier Ga and the lighter B, respectively, are detectable by the employed single-crystal X-ray diffraction analysis.

To highlight the differences among the three structures, the pure MFI data were kept as reference, and the relative site-occupation factors with respect to those of pure MFI, Δ(SOF), were calculated for each T site as follows:

$$\Delta(\text{SOF})(\text{M-MFI}) = \text{SOF (M-MFI)} - \text{SOF (pure MFI)} \quad (4)$$

where M may be B or Ga.

The results are depicted in Figure 6, where the opposite behavior of Ga and B is immediately evident because Ga-MFI always shows positive deviations and B-MFI shows negative deviations, in agreement with the inequality (eq 3). First, this result indicates that a certain degree of random substitution is present. Besides, it is confirmed that framework defects enhance the effects of B insertion and counterbalance the effects of Ga insertion because B-MFI and Ga-MFI present almost the same absolute average ΔSOF value (continuous horizontal lines in Figure 6) even though the difference in atomic number with

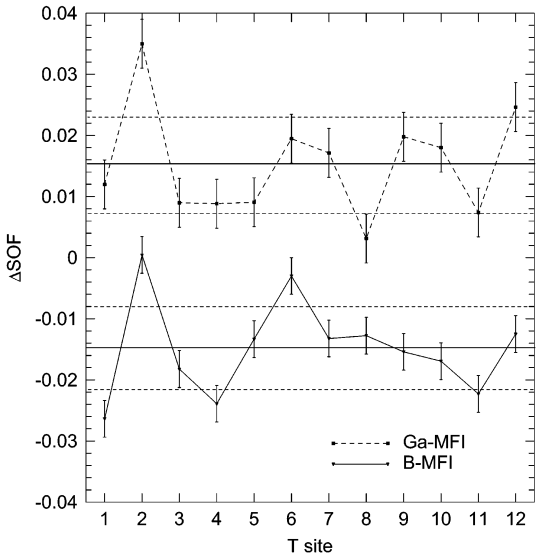

Figure 6. Relative site-occupation factors (ΔSOFs, see eq 3) of the T sites in B- and Ga-MFI with respect to those of pure MFI, obtained from single-crystal X-ray data refinement. The average ΔSOF values (representing a completely random substitution) are indicated by the solid horizontal lines. The dotted horizontal lines indicate the $\pm 2\sigma$ limits.

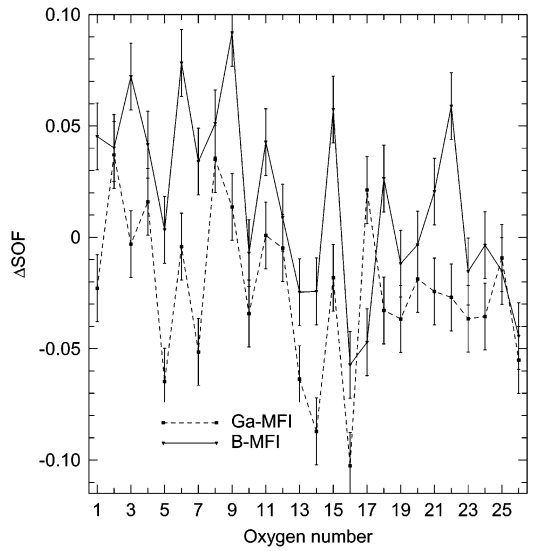

Figure 7. Relative site-occupation factors (ΔSOFs) of the oxygen atoms in B- and Ga-MFI, calculated with respect to those of pure MFI, obtained from the refinement of single-crystal X-ray data. (Oxygen numbers refer to the numbering adopted in ref 42.)

respect to Si is larger for Ga than for B ($\Delta Z = -6$ for B and $+17$ for Ga). To confirm that the changes in the T-site ΔSOFs shown in Figure 6 are really induced by the heteroatom insertion and are not due to systematic errors in the data, we also applied a similar refinement strategy to the SOFs of the oxygen atoms. The resulting ΔSOFs are shown in Figure 7, where it may be immediately seen that the clear repartition of positive and negative ΔSOFs found in Figure 6 does not appear.

Some preferential substitutions are indicated by the sites presenting absolute ΔSOFs with a deviation larger than 2σ (dotted horizontal lines in Figure 6) from the average value (represented by the continuous horizontal lines in Figure 6 and corresponding to totally random substitution). Indeed, T2 (and possibly T12) with a large positive ΔSOF seems to be preferred by Ga. Conversely, T1 (and possibly T4 and T11) with a large negative ΔSOF seems to be preferred by B. Some unfavorable sites for heteroatom insertion are also indicated: T8 (and possibly T11) for Ga and T2 and T6 for B have ΔSOFs very close to zero and should therefore be fully occupied by Si. B and Ga atoms show opposite behavior in the sense that the T2 site preferred by Ga seems unoccupied by B, indicating that this site is more capable of hosting larger atoms. Conversely but only on the borderline limit of 2σ, site T11, which is favored for B, seems to be less occupied by Ga.

By comparing the present single-crystal study with powder diffraction analyses[16,20−22,24,25] with the aim of locating Ti and Fe in the MFI framework, we point out that all of them did not observe the presence of random substitution. Computational studies[19,20] indicate that random substitution should be important because the energy difference for the heteroatom insertion in the different T sites is very small. These results are independent of the adopted computational method and the particular heteroatom employed in the simulation. In this regard, it should be emphasized that a serious limitation of Rietveld refinement from powder data of such a complex structure as MFI is probably the unavoidable use of a common ADP parameter for all Si atoms because of the limited number of independent observations.[52] If we look at the uneven distribution of the single-crystal ADPs in our pure MFI (see Figure 5), then this appears to be a rather crude assumption. The use of a common ADP parameter in all of the Rietveld refinements reported in the literature on substituted MFI[16,20,24,25] could cause a constant biased offset in the refined SOFs of all T sites, erasing the fraction of random distribution and allowing only highly preferential sites (if any) to emerge. Indeed, all groups searched for some reference sample to overcome the "common ADP" limitation and to validate their results: i.e., Artioli et al.[16,24] compared TS-1 to defective silicalite, Hijar et al.,[20] TS-1 to Fe-silicalite (having Ti and Fe opposite neutron scattering factors), and Henry et al.,[25] TS-1 to two isotopically defined TS-1 samples (exploiting the different neutron scattering lengths of the different Ti isotopes). Nevertheless, the possibility of independently refining the ADPs for all T sites seems to be a mandatory strategy in singling out the random substitution phenomenon. Zanardi et al.,[50] employing single-crystal X-ray diffraction data on highly loaded B-FER and B-MFI, were the first to suggest the importance of a B random distribution among the T sites. In the present work, we were able to confirm that a certain degree of random substitution is important, but comparing with pure MFI, taken as a reference material, allowed us to demonstrate that some preferential substitution sites do exist.

4. Conclusions

The good quality of the synchrotron radiation single-crystal data permitted us to shed some light on charge distribution and balance and draw some important conclusions about B and Ga distributions among the T sites in the MFI framework.

The presence in purely siliceous MFI of a residual electron density peak near T9, similar to that found in Fe-MFI, indicated that our previous interpretation, in terms of the Na^+ counterion,[23] had to be revised. The correct suggestion was offered by Fyfe et al.[31] in a recent NMR study indicating the presence of a pentacoordinated SiO_4F^- group at site T9 (Figure 3), which was then confirmed by Aubert et al.[28] The residual electron-density peak found in Fe-MFI, in pure MFI, and also in Ga-MFI at less than 2.0 Å from T9 is due to the fluorine. Indeed, when F^- is taken into account, site T9 assumes a trigonal-bipyramid coordination, and a lengthening of the axial T−O distance opposite to the F^- is expected, in agreement with our observa-

tions (Figure 4). The good quality of the synchrotron data allowed us to locate another less populated peak near T10, which also may be interpreted as a SiO_4F^- group. No similar peak was found near any other T site, confirming that the more-strained T9 and T10 sites, the only ones belonging to a four-member ring in MFI, are preferred by F^-. Site T9 is the most favored for the formation of the SiO_4F^- group because T9 is the site that requires a minimal additional distortion for F insertion. The precise location and the SOF refinement of the extraframework peaks allowed us to shed some light on the distribution of charged species, which contribute to the charge balance in these MFI precursors. In particular, we have demonstrated that the negative charges needed to balance the positive charges of TPA^+ are mainly donated by the F^- bonded to T9 and T10 and by the heteroatoms inserted into the MFI framework. Nevertheless, a small number of disordered groups (hydroxyl groups and/or defects), not detectable in the electron density maps, must be invoked to achieve the neutrality. Finally, we have also shown that fluorine can jump in the cage depicted in Figure 3 between sites F1, F1′, F2, and F2′. Sites F1 and F1′ near T9 are more populated, being less hindered than F2 and F2′ (near 10).

An analysis of the thermal (Figure 5) and occupation factors (Figure 6) of the T sites in the three studied samples (pure MFI and B- and Ga-MFI) indicates that heteroatom insertion in the MFI framework is able to induce subtle but significant changes in the B- and Ga-MFI structures with respect to that of pure MFI. In particular, our data indicate that (i) random substitution is important for both B- and Ga-MFI; (ii) a small but significant degree of preferential substitution does exist: T1 (and possibly T4 and T11) for B and T2 (and possibly T12) for Ga; some sites that are unfavorable for heteroatom substitution exist (T8 and T11 for Ga and T2 and T6 for B); and (iii) B and Ga atoms have different preferred substitution sites, probably because of their opposite behavior as far as their atomic numbers and dimensions with respect to Si are concerned, indicating that preferential substitution sites may also depend on the heteroatom type.

Acknowledgment. This project was supported by MURST (Cofin 2000, Area 03). XRD measurements were performed at the ID11 beamline of the ESRF storage ring within the public user program. The friendly and precious support during data collection by the ID11 staff (and in particular by G. Vaughan and A. Terry) is aknowledged. We are indebted to F. Crea, (University of Calabria), for his help in the synthesis of the samples, A. Zecchina, S. Bordiga, (University of Torino) for critical discussion. L.P. acknowledges an INFM grant for his stay in Grenoble. M.M. acknowledges the "G. Donegani" foundation for a grant in 2001, when these data were collected and analyzed. The stimulating discussions with Dr. E. Aubert (University of Nancy) and with S. Zanardi and A. Alberti (University of Ferrara) are acknowledged.

References and Notes

(1) Flanigen, E. M.; Bennett, J. M.; Grose, R. W.; Cohen, J. P.; Patton, R. L. M.; Kirchner, R.; Smith, J. V. *Nature (London)* **1978**, *272*, 512.

(2) Meier, W. M.; Olson, D. H.; Baerlocher, Ch. *Atlas of Zeolite Structure Types*; Elsevier: London, 1996.

(3) Kokotailo, G. T.; Lawton, S. L.; Olson, G. T.; Meier, W. M. *Nature (London)* **1978**, *272*, 437.

(4) Olson, G. T.; Kokotailo, G. T.; Lawton, S. L.; Meier, W. M. *J. Phys. Chem.* **1981**, *85*, 2238.

(5) Coudurier, G.; Auroux, A. J.; Vedrine, C.; Farlee, R. D.; Abrams, L.; Shannon, R. D. *J. Catal.* **1987**, *108*, 1.

(6) Millini, R.; Perego, G.; Bellussi, G. *Top. Catal.* **1999**, *9*, 13.

(7) (a) Taramasso, M.; Perego, G.; Notari, B. U.S. Patent 4,410,501, 1983. (b) Bordiga, S.; Coluccia, S.; Lamberti, C.; Marchese, L.; Zecchina, A.; Boscherini, F.; Buffa, F.; Genoni, F.; Leofanti, G.; Petrini, G.; Vlaic, G. *J. Phys. Chem.* **1994**, *98*, 4125. (c) Tozzola, G.; Mantegazza, M. A.; Ranghino, G.; Petrini, G.; Bordiga, S.; Ricchiardi, G.; Lamberti C.; Zulian, R.; Zecchina, A. *J. Catal.* **1998**, *179*, 64. (d) Millini, R.; Previde Massara, E.; Perego, G.; Bellussi, G. *J. Catal.* **1992**, *137*, 497. (e) Ricchiardi, G.; Damin, A.; Bordiga, S.; Lamberti, C.; Spanò, G.; Rivetti, F.; Zecchina, A. *J. Am. Chem. Soc.* **2001**, *123*, 11409. (f) Bordiga, S.; Damin, A.; Bonino, F.; Ricchiardi, G.; Lamberti, C.; Zecchina, A. *Angew. Chem. Int. Ed.* **2002**, *41*, 4734.

(8) (a) Bayese, C. R.; Kentgens, A. P. R.; de Haan, J. W.; van de Ven, L. J. M.; van Hooff, J. H. C. *J. Phys. Chem.* **1992**, *96*, 755. (b) Liu, X.; Klinowski, J. *J. Phys. Chem.* **1992**, *96*, 3403. (c) Otero Areán, C.; Turnes Palomino, G.; Geobaldo, F.; Zecchina, A. *J. Phys. Chem.* **1996**, *100*, 6678. (d) Lamberti, C.; Turnes Palomino, G.; Bordiga, S.; Zecchina, A.; Spanò, G.; Otero Areán, C. *Catal. Lett.* **1999**, *63*, 213.

(9) Fricke, R.; Kosslick, H.; Lischke, G.; Richter, M. *Chem. Rev.* **2000**, *100*, 2303.

(10) (a) Szostak, R.; Thomas, T. L. *J. Catal.* **1986**, *100*, 555. (b) Bordiga, S.; Buzzoni, R.; Geobaldo, F.; Lamberti, C.; Giamello, E.; Zecchina, A.; Leofanti, G.; Petrini, G.; Tozzola, G.; Vlaic, G. *J. Catal.* **1996**, *158*, 486. (c) Geobaldo, F.; Lamberti, C.; Bordiga, S.; Zecchina, A.; Turnes Palomino, G.; Otero Areán, C. *Catal. Lett.* **1996**, *42*, 25. (d) Berlier, G.; Spoto, G.; Bordiga, S.; Ricchiardi, G.; Fisicaro, P.; Zecchina, A.; Rossetti, I.; Selli, E.; Forni, L.; Giamello, E.; Lamberti, C. *J. Catal.* **2002**, *208*, 64.

(11) (a) Szostak, R. *Molecular Sieves*; Van Nostrand Reinhold: New York, 1989; p 205. (b) Sulikowski, B. *Heterog. Chem. Rev.* **1996**, *3*, 203.

(12) (a) Chu, C. T.-W.; Chang, C. *J. Phys. Chem.* **1985**, *89*, 1569. (b) Strodel, P.; Neyman, K. M.; Knötzinger, H.; Rösch, N. *Chem. Phys. Lett.* **1995**, *240*, 547. (c) Stave, M. S.; Nicholas, J. B. *J. Phys. Chem.* **1995**, *99*, 15046. (d) Parrillo, D. J.; Lee, C.; Gorte, R. J.; White, D.; Farneth, W. E. *J. Phys. Chem.* **1995**, *99*, 8745.

(13) Vezzalini, G.; Quartieri, S.; Galli, E.; Alberti, A.; Cruciani, G.; Kvick, Å. *Zeolites* **1997**, *19*, 323.

(14) (a) Zecchina, A.; Bordiga, S.; Spoto, G.; Marchese, L.; Petrini, G.; Leofanti, G.; Padovan, M. *J. Phys. Chem.* **1992**, *96*, 4985. (b) Zecchina, A.; Bordiga, S.; Spoto, G.; Marchese, L.; Petrini, G.; Leofanti, G.; Padovan, M. *J. Phys. Chem.* **1992**, *96*, 4991.

(15) (a) Zecchina, A.; Bordiga, S.; Spoto, G.; Marchese, L.; Petrini, G.; Leofanti, G.; Padovan, M.; Otero Areàn, C. *J. Chem. Soc., Faraday Trans.* **1992**, *88*, 2959. (b) Marra, G. L.; Tozzola, G.; Leofanti, G.; Padovan, M.; Petrini, G.; Genoni, F.; Venturelli, B.; Zecchina, A.; Bordiga, S.; Ricchiardi, G. *Stud. Surf. Sci. Catal.* **1994**, *84*, 559.

(16) Artioli, G.; Lamberti, C.; Marra, G. L. *Acta Crystallogr., Sect. B* **2000**, *56*, 2.

(17) (a) Bordiga, S.; Roggero, I.; Ugliengo, P.; Zecchina, A.; Bolis, V.; Artioli, G.; Buzzoni, R.; Marra, G. L.; Rivetti, F.; Spanò, G.; Lamberti, C. *J. Chem. Soc., Dalton Trans.* **2000**, 3921. (b) Bordiga, S.; Ugliengo, P.; Damin, A.; Lamberti, C.; Spoto, G.; Zecchina, A.; Spanò, G.; Buzzoni, R.; Dalloro, L.; Rivetti, F. *Top. Catal.* **2001**, *15*, 43. (c) Bolis, V.; Busco, C.; Bordiga, S.; Ugliengo, P.; Lamberti, C.; Zecchina, A. *Appl. Surf. Sci.* **2002**, *196*, 56.

(18) Oumi, Y.; Matsuba, K.; Kubo, M.; Inui, T.; Miyamoto, A. *Microporous Mater.* **1995**, *4*, 53.

(19) (a) Jentys, A.; Catlow, C. R. A. *Catal. Lett.* **1993**, *22*, 251. (b) Millini, R.; Perego, G.; Seiti, K. *Stud. Surf. Sci. Catal.* **1994**, *84*, 2123. (c) Smirnov, K. S., van de Graaf, B. *Microporous Mater.* **1996**, *7*, 133. (d) Njo, S. L.; van Koningsveld, H.; van de Graaf, B. *J. Phys. Chem. B* **1997**, *101*, 10065. (e) Ricchiardi, G.; de Man, A.; Sauer, J. *Phys. Chem. Chem. Phys.* **2000**, *2*, 2195.

(20) Hijar, C. A.; Jacubinas, R. M.; Eckert, J.; Henson, N. J.; Hay, P. J.; Ott, K. C. *J. Phys. Chem. B* **2000**, *104*, 12157.

(21) Lamberti, C.; Bordiga, S.; Zecchina, A.; Carati, A.; Fitch, A. N.; Artioli, G.; Petrini, G.; Salvalaggio, M.; Marra, G. L. *J. Catal.* **1999**, *183*, 222.

(22) Marra, G. L.; Artioli, G.; Fitch, A. N.; Milanesio, M.; Lamberti, C. *Microporous Mesoporous Mater.* **2000**, *40*, 85.

(23) Milanesio, M.; Lamberti, C.; Aiello, R.; Testa, F.; Piana, M.; Viterbo, D. *J. Phys. Chem. B* **2000**, *104*, 9951.

(24) Lamberti, C.; Bordiga, S.; Zecchina, A.; Artioli, G.; Marra, G. L.; Spanò, G. *J. Am. Chem. Soc.* **2001**, *123*, 2204.

(25) Henry, P. F.; Weller, M. T.; Wilson, C. C. *J. Phys. Chem. B* **2001**, *105*, 7452.

(26) Testa, F.; Crea, F.; Aiello, R.; Nagy, J. B. *Stud. Surf. Sci. Catal.* **1999**, *125*, 165.

(27) Fonseca, A.; Nagy, J. B.; El Hage-Al Asswad, J.; Mostowicz, R.; Crea, F.; Testa, F. *Zeolites* **1995**, *15*, 259−263.

(28) Aubert, E.; Porcher, F.; Souhassou, M.; Dusausoy, Y.; Lecomte, C. *J. Phys. Chem.* **2002**, *106*, 1110.

(29) Note that both Aubert et al.[28] and Fyfe et al.[31] refer to a $SiO_{4/2}F^-$ structure, so recalling that each oxygen atom is shared by two silicon atoms.

(30) Koller, H.; Wölker, A.; Villaescusa, L. A.; Diaz-Cabanas, J.; Valencia, S.; Camblor, M. A. *J. Am. Chem. Soc.* **1999**, *121*, 3368.

(31) Fyfe, C. A.; Brouwer, D. H.; Lewis, A. R.; Chezeau, J. M. *J. Am. Chem. Soc.* **2001**, *123*, 6882.

(32) Geus E. R.; van Bekkum, H. F. *Zeolites* **1995**, *15*, 333.

(33) (a) Palin, L. Degree Thesis in Material Science, University of Torino, Torino, Italy, 2001. Palin, L.; Milanesio, M.; Viterbo, D.; Marra, G. L.; Testa, F.; Aiello, R.; Lamberti, C. To be submitted for publication.

(34) Testa, F.; Chiappetta, R.; Crea, F.; Aiello, R.; Fonseca, A.; Nagy, J. B. *Colloid Surf., A* **1996**, *115*, 223.

(35) Nigro, E.; Crea, F.; Testa, F.; Aiello, R.; Lentz, P.; Nagy, J. B.; *Microporous Mesoporous Mater.* **1999**, *30*, 199.

(36) Price, G. D.; Pluth, J. J.; Smith, J. V.; Bennett, J. M.; Patton, R. L. *J. Am. Chem. Soc.* **1982**, *104*, 5971−5977.

(37) Weidenthaler C.; Fischer, R. X.; Shannon, R. D.; Medenbach, O. *J. Phys. Chem.* **1994**, *98*, 12687−12694.

(38) The availability of very good synchrotron diffraction data from twin crystals of pure MFI allowed us to use these data to test our procedure for separating the contributions of the two individuals of the merohedral twin to the overall intensities. The need for this separation procedure arose from our attempt to use Ga anomalous scattering for its localization in the MFI framework.

(39) Viterbo, D.; Milanesio, M.; Palin, L.; Lamberti, C. Proposal CH1027, Beamline ID11 at the ESRF (http://www.esrf.fr/exp_facilities/ID11/handbook/).

(40) *SMART*; Bruker AXS, Inc.: Madison, WI, 1998.

(41) *SAINT*; Bruker AXS, Inc.: Madison, WI, 1994−1996.

(42) Van Koningsveld, H.; Van Bekkum, H.; Jansen, J. C. *Acta Crystallogr., Sect. B* **1987**, *34*, 127.

(43) Sheldrick G. M. *SHELXL-97*; University of Göttingen: Göttingen, Germany, 1997 (http://shelx.uni-ac.gwdg.de/SHELX/).

(44) Ugliengo, P.; Viterbo, D.; Chiari, G. *Z. Kristallogr.* **1993**, *207*, 9.

(45) Millini, R.; Perego, G.; Berti, D.; Parker Jr, W. O.; Carati, A.; Bellussi, G. *Microporous Mesoporous Mater.* **2000**, *35*−*36*, 387.

(46) Newsam, J. M.; Vaughan, D. E. W. In *New Developments in Zeolite Science and Technology*, Proceedings of the 7th International Zeolite Conference, Tokyo, Japan, Aug 17−22, 1986; Murakami, Y., Iijima A., Ward, J. W., Eds.; Kodansha-Elsevier: Tokyo, 1986.

(47) Larson, A. C.; Von Dreele, R. B. *General Structure Analysis System (GSAS)*; Report LAUR 86-748 (2000); Los Alamos National Laboratory: Los Alamos, NM, 2000; pp 86−748 (http://www.ccp14.ac.uk/solution/gsas/index.html).

(48) George, A. R.; Catlow, C. R. A. *Zeolites* **1997**, *18*, 67.

(49) Bordiga, S.; Damin, A.; Bonino, F.; Zecchina, A.; Spanò, G.; Rivetti, F.; Bolis, V.; Prestipino, C.; Lamberti, C. *J. Phys. Chem. B* **2002**, *106*, 9892.

(50) (a) Zanardi, S.; Alberti, A.; Millini, R.; Bellussi, G.; Perego, G. *Stud. Surf. Sci. Catal.* **2002**, *142*, 1923. (b) Perego, G.; Bellussi, G.; Millini, R.; Alberti, A.; Zanardi, S. *Microporous Mesoporous Mater.* **2002**, *56*, 193.

(51) Periodic ab initio calculations on siliceous chabazite at the Hartree−Fock level result in a Mulliken charge on the Si atoms of $+2.0|e|$ (Damin, A.; Bordiga, S.; Zecchina, A.; Lamberti, C.; Doll, K. *J. Chem. Phys.*, in press. Ab initio calculations on a large siliceous cluster ($Si_{18}O_{26}H_{20}$) resulted in a Mulliken charge on the central Si atom of $2.0|e|$ or 2.2 depending on the adopted Hamiltonian (B3-LYP or Hartree−Fock) (Damin, A.; Bordiga, S.; Zecchina, A.; Lamberti, C. *J. Chem. Phys.* **2002**, *117*, 226).

(52) Altomare, A.; Cascarano, G.; Giacovazzo, C.; Guagliardi, A.; Moliterni, A. G. G.; Burla, M. C.; Polidori, G. *J. Appl. Crystallogr.* **1995**, *28*, 738.